Joint Optimization of HVAC and Active Insulation Control Strategies in Residential Buildings

Amin Sepehri[a,1,*], Gregory S. Pavlak[a,1,2]

[a] *The Pennsylvania State University, 104 Engineering Unit A, University Park, PA 16802, USA*

Abstract

Recently, active insulation systems (AIS) have been conceptualized in building envelopes to optimally modulate the thermal resistance in response to changing environmental conditions. Building flexibility can further be improved if the building is also equipped with optimized heating, ventilating, and air conditioning (HVAC) control. In this work, we investigate the annual potential benefits of jointly optimizing AIS and HVAC system controls in both heating and cooling days over all climate zones (CZs) in the U.S. To reduce the computational complexity of applying model predictive control (MPC) to annual operations and detailed whole-building energy models, timeseries clustering was used to identify a set of representative days for optimizing in each climate zone. To isolate the increase in benefits from this joint optimization, we compare the performance to cases where the AIS and HVAC controls are optimized separately. Results indicate savings potential in all CZs, with the largest annual average savings of 9.02% and 4.02% observed in the cooling days with large daily temperature swings and heating days with cold sunny condition, respectively. Savings patterns across climate zone, day types, and HVAC mode (i.e., heating or cooling) are also discussed along with the implications of important system design variables.

Keywords: Active Insulation, Model Predictive Control, Stochastic Optimization, Thermal Energy Storage, Transactive Control, Uncertainty quantification

1. Introduction

Buildings account for over one-third of global energy consumption and 40% of total direct and indirect carbon emissions [1]. Hence, encouraging efficient use of energy in buildings plays a critical role in reducing total energy use and greenhouse gas emissions. While increasing resistance in building construction has been shown to be an effective traditional way of improving building energy efficiency, it has resulted in static thermal behavior that can be prone to overheating and neglects the dynamics of electric power systems due

*Corresponding author
Email addresses: afs6101@psu.edu (Amin Sepehri), gxp93@psu.edu (Gregory S. Pavlak)
[1]Department of Architectural Engineering
[2]Penn State Institutes of Energy and the Environment

to the increasing integration of wind and solar resources, which are variable in nature. With the advent of AIS, though, there is an opportunity to achieve energy efficiency and grid-responsiveness while improving occupant comfort.

With continued integration of variable renewable generations to the grid, considering the three general impacts of buildings on the grid (i.e., total energy use, peak demand, and timing of energy use) is of great importance. According to the U.S. Department of Energy, around 40% of the total energy used by buildings is consumed by HVAC systems [2]. To address the three aforementioned impacts of building load on the electric grid, demand response programs, such as load shedding and shifting, have been introduced to leverage building thermal mass to reshape building load profiles via precooling and preheating using HVAC systems.

Compared to HVAC setpoint control, AIS control presents a new possibility for leveraging building thermal mass, and optimal control of both technologies can ultimately lead to Grid-interactive Efficient Buildings (GEBs). As stated in a roadmap report by the U.S. Department of Energy Building Technologies Office [3], GEBs are energy-efficient buildings with smart technologies characterized by the active use of distributed energy resources (DERs) to provide demand flexibility while co-optimizing for energy cost, grid services, and occupant needs, in a continuous and integrated way. Thus far, literature has confirmed the ability of HVAC preconditioning in achieving load flexibility in GEBs. Also, studies like Shekar and Krarti [4] have verified the same ability for AIS by selecting the right thermal resistances. AIS and HVAC controls had typically been decoupled, but recently Cui et al. [5] applied MPC to four simplified thermal resistance-capacitance (RC) models and reported large amounts of savings by coupling the two technologies. This work was able to highlight the potential benefits of jointly optimizing AIS and HVAC systems, but the baseline controller did not allow for separation of the savings contributions of each technology individually. In addition, no study thus far has provided a comprehensive evaluation of the joint optimization using detailed-whole building energy models across both heating and cooling seasons and representative U.S. climate zones.

In this work, we extend the literature on analyzing optimal control of AIS and HVAC systems by systematically comparing the savings of the AIS-only, HVAC-only, and jointly optimized cases. The comparison is made across U.S. climate zones, and for a full year of weather conditions. This analysis allows for insight into when and where each of the technologies (i.e, AIS-only, HVAC-only, and both) may be most beneficial. Section 2 provides additional context through the review of relevant literature. Section 3 describes the building models used in this study, optimization environment, and performance comparison scheme. Section 4 provides results of the study, followed by closing remarks in Section 5.

2. Background

Over the past thirty years, researchers have evaluated the use of building thermal capacitance to reduce costs and energy use. Through optimal control of the intrinsic thermal storage within building structures, Braun [6] showed the potential ability to reduce energy costs and the peak demand up to 50% and 35% respectively. Rabl and Norford [7] showed that preconditioning buildings at night could reduce peak demand during the day. Morris et al. [8] considered two optimal dynamic control strategies including minimum total energy costs and minimum peak electrical demand and reported the ability to shift 51% of the total cooling load to off-peak or a reduction of 40% in the peak cooling load of a large office building. Keeney and Braun [9] investigated the application of precooling in a 1.4 million square foot office building in Hoffman Estates, IL, to reduce the chiller peak load by 25%. Florita et al. [10] developed an optimal passive thermal-mass control simulation environment to minimize total utility cost, including both energy and demand charges.

Recently, the benefits of Model Predictive Control (MPC), as an optimization framework to control HVAC have been proven among researchers [11]. For instance, Ma et al. [12] demonstrated the effectiveness of MPC to reduce demand and energy costs under time-of-use energy pricing and Greensfelder et al. [13] examined the cost savings potential of optimal precooling of thermal mass under real-time pricing. Olivieri et al. [14] evaluated short-term demand curtailment in a commercial building using building thermal inertia. On the other hand, some researchers have even found it a suitable substitute for traditional approaches like PIDs that only focused on indoor air conditioning [15, 16]. However, MPC is not yet able to play a stand-alone role in buildings due to several issues including privacy and cyber-security, availability of appropriate hardware and software infrastructure, lack of trained personnel for commissioning and maintenance, along with others mentioned by Drgoňa et al. [11]. MPC can also work well when thermal energy storage, such as passive building thermal mass or active storage systems, is considered in the problem [17]. Thus, MPC is implemented in this study to drive the passive thermal storage of buildings.

In separate work, researchers have also shown that excessive construction insulation can cause thermal discomfort during summer due to overheating in [18, 19, 20]. Active insulation systems have been introduced to enable the thermal characteristics of the envelope to be more dynamic, and Park et al. [21] reported average reductions of 15% and 10% in annual cooling and heating energy use, respectively, using a simplified two-step control strategy for AIS in residential buildings. In addition, dynamic insulation has also been paired with phase change materials (PCM), since it harnesses PCM latent heat during a complete phase change process [22].

So far, miscellaneous approaches have been taken to reach the same AIS behavior. For instance, Kimber et al. [23] presented a multilayered wall that could switch from a conductive to an insulated state by positioning thin polymer membranes within a wall to create stagnant air. Breathing wall is another common approach based on convection (air) to reduce energy consumption in buildings while ensuring a proper Indoor

Air Quality (IAQ) by providing enough outdoor air into the building for ventilation purposes. According to Imbabi [24], it is an ideal solution for both new buildings and retrofit applications. Another insulation type based on convection (air) is translucent façade elements. Pflug et al. proposed a translucent insulation panel that is moved vertically or rolled up/down between two fixed layers to switch between the insulating and conducting states by switching the wall U-value [25, 26, 27]. Unlike breathing walls, they showed large improvements in the summer thermal comfort in addition to a cooling demand reduction of 29.6%.

Thermal diodes are another way of achieving AIS. Varga et al. [28] worked on a numerical solution of the heat transfer problem to characterize thermophysical properties (i.e., conductivity, diffusivity, and specific heat) of a thermal diode in a heat pipe panel. They showed that the thermal diode conductivity could be altered by three to five times between the forward and backward heat transfer. The last mechanism covered in this literature review is differing gas pressure inside a vacuum insulation panel. Benson et al. [29] designed variable-conductance vacuum insulation (VCI) which used an electronic heater to change the temperature of the hydride. Once the temperature was changed, hydrogen adsorption and desorption provided the lower and upper limits of the insulation layer.

Most of the aforementioned technologies are either conceptual or only tested as prototypes. However, researchers have utilized simulation tools to evaluate the effects of AIS by controlling the solid-state conductivity. Developing a simulation strategy, Favoino et al. [30] showed the potential of AIS to reduce building energy use, followed by Jin et al.'s work [31] which showed an annual energy saving potential of 50%. Menyhart and Krarti [32] used a modified RC model to simulate the AIS control mechanism with two steps (low-R and high-R). They reported a potential range of total energy savings of 7% to 42% compared to a baseline with static insulation. Shekar and Krarti [4] expanded on this work by optimizing the R-value by a genetic algorithm in an office building and reported a maximum potential saving of 17% in annual heating and cooling energy costs.

While all of those studies have estimated the potential reductions in total energy use, Antretter et al. [33] used the Energy Management System (EMS) feature of EnergyPlus to develop a rule-based control algorithm to model AIS and illustrated a flexible control of charging and discharging of AIS from both exterior and interior sides of a wall. They showed that such control could then result in a dynamic building energy management that has the potential to provide grid services like load shedding and shifting. Expanding on the last work, Mumme et al. [34] showed a smarter building envelope by coupling thermal storage to AIS. They also claimed a more flexible building envelope when AIS is accompanied by pre-conditioning. However, neither the AIS control nor the pre-conditioning schedule was operationally optimized. Using a time-varying MPC controller based on resistance-capacitance thermal network models, Cui et al. [5] simultaneously optimized AIS and HVAC schedules within two optimization scenarios. Scenario 1 aimed to minimize electric energy consumption while scenario 2 tried to minimize the electric cost. The MPC controller resulted in large savings when compared to a two-position (i.e., ON/OFF) rule-based controller

with a 2 °C switching differential. The benefits of joint optimization of AIS and HVAC systems were highlighted, however, the study did not explore the savings contributions of each technology individually.

In our earlier study [35], we used a detailed-whole building energy model to jointly optimize AIS and HVAC controls within an MPC framework. We developed a cost function to minimize the peak demand and the energy consumption at the same time. As a result, we observed a total savings of 10% in the cost function with 3% energy savings and 13% peak demand reduction. In other words, the complementary behavior between the two technologies revealed notable savings with interestingly no enforced penalty in the total energy consumption. Still, that study was limited to a single day, building type, and climate zone of 4A for Baltimore, MD. Thus, future exploration was needed to more thoroughly evaluate the technologies.

To the best of our knowledge, no other work thus far has comprehensively evaluated the joint optimization of HVAC setpoint and AIS controls using detailed-whole building energy models to accurately account for time-varying internal and external disturbances and heat transfer processes, across both heating and cooling seasons and multiple climate zones. Therefore, in this work, we extended our earlier model to quantify potential savings for the range of annual weather conditions for the prototype building in representative U.S. climate zones. An intricate comparison of the savings to the AIS- and HVAC-only approaches is also provided to better understand the potential interactions and synergies between the two technologies in all climate conditions.

3. Methods

To quantitatively evaluate the benefit of jointly optimizing building HVAC operations and dynamic envelope properties a framework was developed that couples detailed whole-building energy models with optimization algorithms to generate optimal control decisions for the proposed systems. The following subsections provide more detail on the building energy models used in this study, and the components of the optimization framework.

3.1. Building Models

The single-family DOE (Figure 1) residential prototype building with net conditioned area of 220.82 m^2 (2377 ft^2) are used as baseline models for each climate zone (CZ). Table 1 provides more detail about the location of each building with the corresponding CZ. Heating and cooling are provided by all-electric heat pump systems with heating and cooling setpoints of 20 °C and 24 °C, respectively. The baseline exterior wall construction is similar to our earlier work [35], originally adopted from Antretter et al. [33] to include thermal mass (concrete 140 mm (5.51 in)) between two insulation layers. Two insulation layers satisfy the total R-value required by IECC 2012 in each CZ. The outside wall layer is covered by cladding stucco (10 mm (0.4 in)), and the inside layer is Gypsum board (10 mm (0.4 in)).

Table 1: Location details of the DOE prototype buildings. Degree days are computed relative to a base of 65°F [36] and average temperatures are based on the latest 15-year period (2006-2020) [37].

CZ	Location	Annual Max [°C]	Annual Min [°C]	Annual Avg. [°C]	Heating Degree Days [°C]	Cooling Degree Days [°C]
1A	Miami, FL	27	22	25	30	2777
2A	Tampa, FL	28	19	24	173	2237
3B	El Paso, TX	26	12	19	1213	1686
4A	New York, NY	17	9	13	2573	763
5A	Buffalo, NY	14	5	10	3721	335
6A	Rochester, NY	15	5	10	3603	348
7	Int Falls, MN	9	-3	3	5751	116
8	Fairbanks, AK	4	-7	-2	6567	65

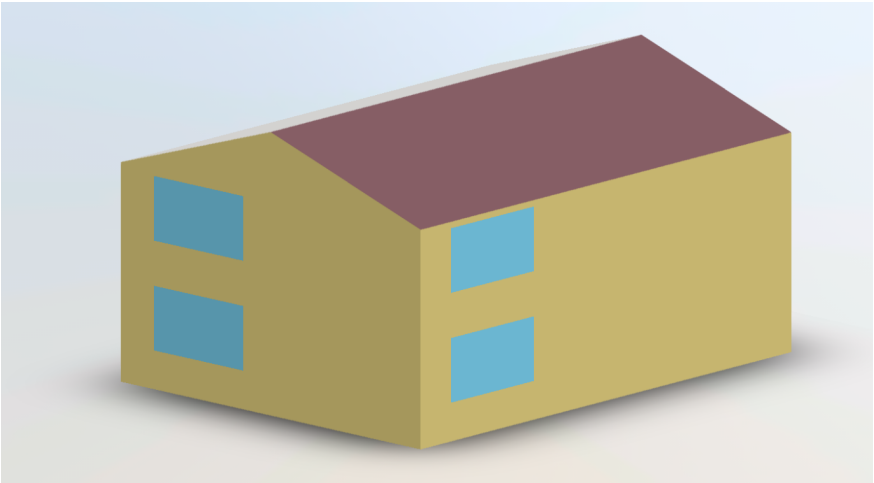

Figure 1: The single-family DOE residential prototype building

There are five AIS configurations that are considered in this work (Figure 2). While the baseline model is always at configuration 4 with both the interior and exterior insulation layers in the On state (i.e., On-On), the optimizer can choose any configuration from 1 to 4. Configuration 3 means the exterior layer is Off while the interior layer is On (i.e, Off-On), configuration 2 (i.e, On-Off) is the opposite case 3, and configuration 1 (i.e, Off-Off) is with both layers at Off state with total insulation resistance of only $0.007\,\mathrm{m^2\,K\,W^{-1}}$. Configuration 5 resembles configuration 2 with On-Off structure. While configuration 5 satisfies the total required R-value at the exterior layer, configuration 2 had the total resistance split between the interior and exterior layers. As a result, configuration 5 allows all thermal mass to be available for preconditioning

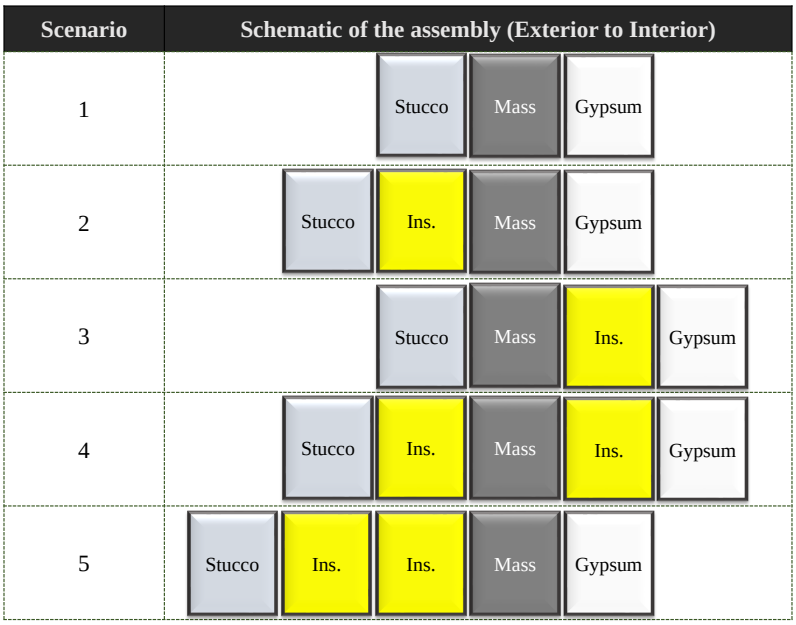

Figure 2: Wall constructions used to simulate the range of AIS states. The core Mass is concrete 140 mm (5.51 in), Stucco represents cladding stucco 10 mm (0.4 in), and Gypsum board is 10 mm (0.4 in)

of the space via HVAC control in addition to having full insulation, which makes it more suitable for the HVAC-only case study to assess the maximum power of HVAC system to precool the thermal mass. In other words, it makes the mass fully accessible for charging/discharging via changes in zone air temperature.

3.2. Annual Time Series Reduction

TMY3 EPW weather data are used to simulate the EnergyPlus prototypes. To reduce the computational burden of a whole year optimization in each CZ, a clustering problem is solved on the building surface temperature to identify similar groups of days for the baseline EnergyPlus model in an year. Clustered days are then considered as the representative days of the CZ and optimization problems are only solved on those days. Hence, MPC is applied to four to six days of the year (instead of 365), which significantly reduces the computational time needed to run MPC in that CZ.

After investigating possible candidates, it was decided that the outside surface temperature of the south facing wall a suitable timeseries for performing the clustering. The surface temperature is believed to be the best indicator of the AIS system decision as it includes the combined effect of solar radiation, radiant, and convective heat transfer to the wall. In other words, if the surface temperature is high, AIS should block the heat coming from the wall in a cooling day or facilitate the heat flow in a heating day.

Time series clustering is performed in each CZ using the agglomerative hierarchical method. Figure 3 illustrates four clusters found for CZ 5A including the surface temperature in the top row, followed by the outdoor drybulb temperature in the middle, and direct solar radiation in the bottom. While the clustering

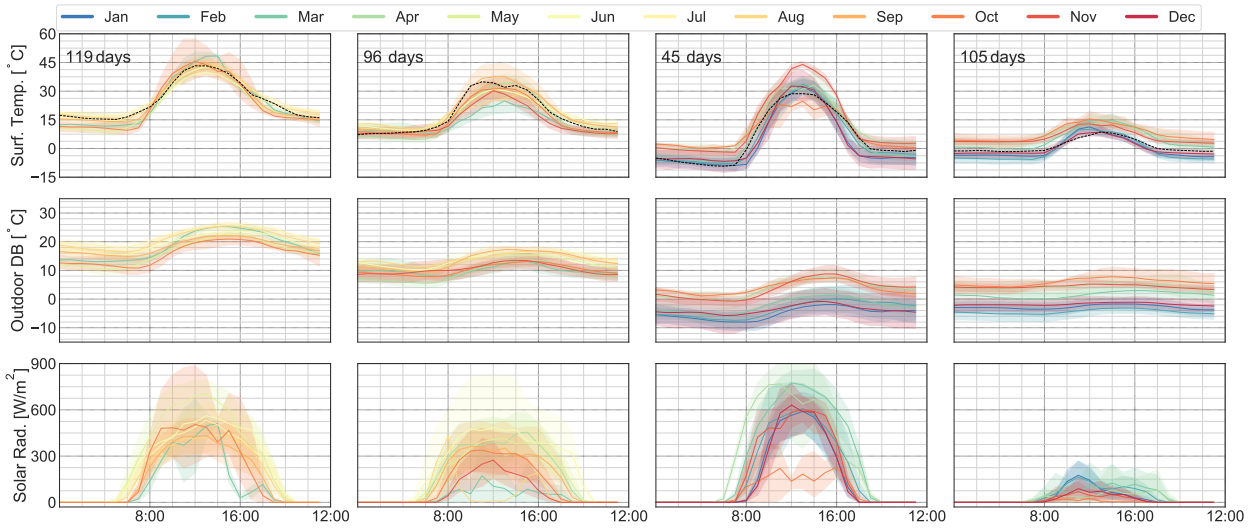

Figure 3: Outside wall surface temperature clustering for Buffalo, NY from climate zone 5A - Black dashed lines are the set of representative days for four clusters of this climate zone.

was done on surface temperature, the last two rows are provided to help in interpreting the clustered days. As a result, we can generally consider each column from left to right as: hot days cool nights, cool cloudy days, cold sunny days, and cold cloudy days of the year in CZ 5A. Applying the euclidean distance metric, the centroid for each each cluster was found and is shown in the black dashed lines in each cluster. Optimization problems were then solved for each representative day to determine the potential savings for each cluster. For instance, June 30 is found as the centroid day of the first cluster with 119 hot and sunny days and thus the MPC is optimized for that particular day.

3.3. Optimization Environment

A MPC framework is applied in this study through a variant of the metaheuristic particle swarm optimization (PSO) algorithm for optimizing AIS and HVAC operations. The algorithm generates a candidate control vector as candidate solutions (particles) and expects the cost of that control strategy to be returned by a function evaluator. Based on the cost, the PSO algorithm moves the particles around in the search space using position and velocity updates to determine the next candidate solutions to try. The local best variant of PSO is used from the PySwarms optimization package [38]. The optimization problem to be solved is the minimization of a blended cost function of energy and peak demand as described in Eq. (1) below.

$$\min_{T_{setpoint,AIS}} \left(\sum_{t=1}^{24} E_{cooling} * w_1 + \max(E_{cooling,4pm-7pm}) * w_2\right) \tag{1}$$

$$s.t. \quad 20\ ^{\circ}\text{C} \leq T_{setpoint}(t) \leq 24\ ^{\circ}\text{C} \ \ \forall t \in \{1...24\} \tag{2}$$

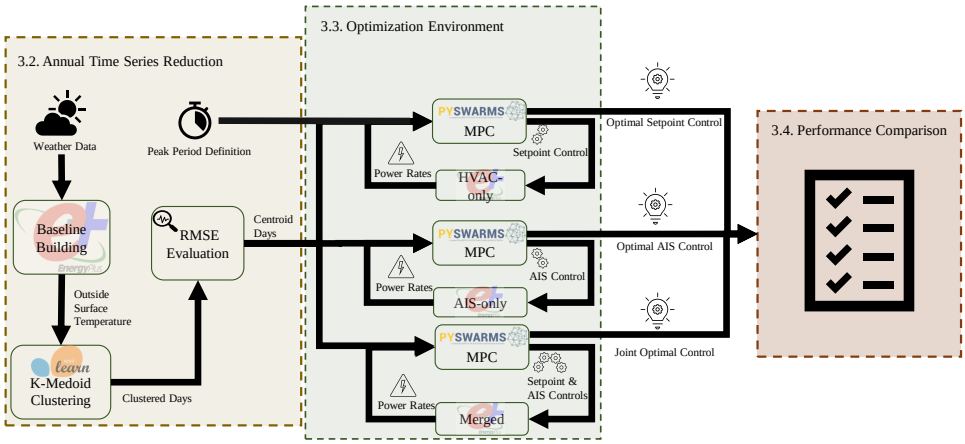

Figure 4: Methods Layout - after determining the centroid days in Subsection 3.2, MPC optimizations are solved per Subsection 3.3. Optimal controls are then compared as described in Subsection 3.4.

$$AIS(t) \in \{1, 2, 3, 4\} \quad \forall t \in \{1...24\} \tag{3}$$

where $E_{cooling}$ is energy use associated with the cooling system in kW, w_1 is the weighting factor corresponding to the daily energy use component, w_2 is the weighting factor corresponding to the peak of energy use from 4 to 7 pm, $T_{setpoint}$ is the cooling HVAC setpoint temperature in °C, and AIS is the AIS configuration state. The optimization cost function is set to minimize the peak demand in addition to the total building cooling energy by varying the cooling setpoint temperature within the upper and lower bounds (Eq. (2)) and the AIS configuration among the four possible states as in Eq. (3). In order to maintain a 70%-30% weighting for the energy consumption and the peak demand, respectively, w_1 and w_2 are chosen 0.022 and 1 in this study. Hence, as the optimizer reduces the cost function, more necessity is given to the peak demand reduction than minimizing the energy consumption. The values were chosen to encourage energy efficient attainment of substantial peak demand reduction.

As shown in Figure 4, HVAC and AIS schedules are determined by the optimizer for each centroid day using a peak period definition. The optimizer is equipped with scripting language for Energyplus (i.e. Eppy [39]) to modify and read idf files and output files. In each time step, after 100 different schedules, known as particles, are imposed in idf file by eppy, EnergyPlus simulations begin. Two primary output variables are then sent back to the optimizer for post-processing, creating a loop between the EnergyPlus and the optimizer to find the best next 100 particles within 100 iterations. While HVAC schedule is directly managed by eppy, the AIS schedule needs to follow an EnergyPlus Energy Management System (EMS) procedure until the right configurations are assigned in EnergyPlus. That procedure includes three main objects in EnergyPlus including EnergyManagmentSystem:Sensor, EnergyManagmentSystem:Program, and

EnergyManagmentSystem:Actuator. First, Sensor receives an imposed AIS schedule from the optimizer. After the schedule is read by the EMS Program to determine what action (i.e. configuration) to take, Actuator initiates the action and switch the desired configuration on the surrounding walls.

3.4. Performance Comparison

Three case studies are included in this study: HVAC-only, AIS-only, and HVAC+AIS (i.e., Merged case). Zone temperature setpoints are optimized in the HVAC-only case. AIS insulation ON/OFF states are optimized in the AIS-only case. The Merged case jointly optimizes the 24-hour profile of zone temperature setpoints and AIS states. The performances are compared to a baseline case with no preconditioning and no AIS control on the clustered days to compute the percent savings. By comparing savings across these three cases (with respect to the same baseline), we can isolate the individual savings of each technology before presenting the combined savings to show the potentially complementary or synergistic nature.

4. Results and Discussion

We first present the overall savings for the merged case across climate zones in Subsection 4.1, followed by a comparison of savings across technologies in Subsection 4.2. The details of daily operations for stand-out cases are highlighted in Subsections 4.5 - 4.6.

4.1. Comparison of Merged Case Across Climate Zones

The overall savings results for all climate zones are presented in Figure 5. Each column in the grid of figures represents a climate zone, and the rows are different clusters. To better observe patterns and compare the savings across different climate zones, the surface temperatures are shown with the savings annotations and the daily profiles were color coded based on the temperature conditions. For example, days where the building exterior surface temperatures are high during both the daytime hours and night time hours occur in CZ1A, CZ2A, CZ3B, and CZ4A. Also shown on each subfigure is the number of days that are part of that specific cluster in a given climate zone. As one would expect, CZ1A has many more days with hot days and nights than the other climate zones. The color legend in Figure 5 also displays the average savings among the days in a particular color group. For example, the average savings for days with both hot days and nights was 1.47%.

As mentioned above, the daily profiles in Figure 5 are color coded based on the temperature conditions. Within each color code, there exists multiple days that are similar to each other even from different CZs. In other words, savings within the color coded categories tend to be in fairly good agreement. As expected, moving from CZ1A to CZ4A, there are fewer days with both hot days and hot nights (i.e. yellow category) until no day from CZ5A appears in the same category. Hot days and cool nights are shown in green and appears in all CZs. The most significant savings during the cooling days occurred in this category with

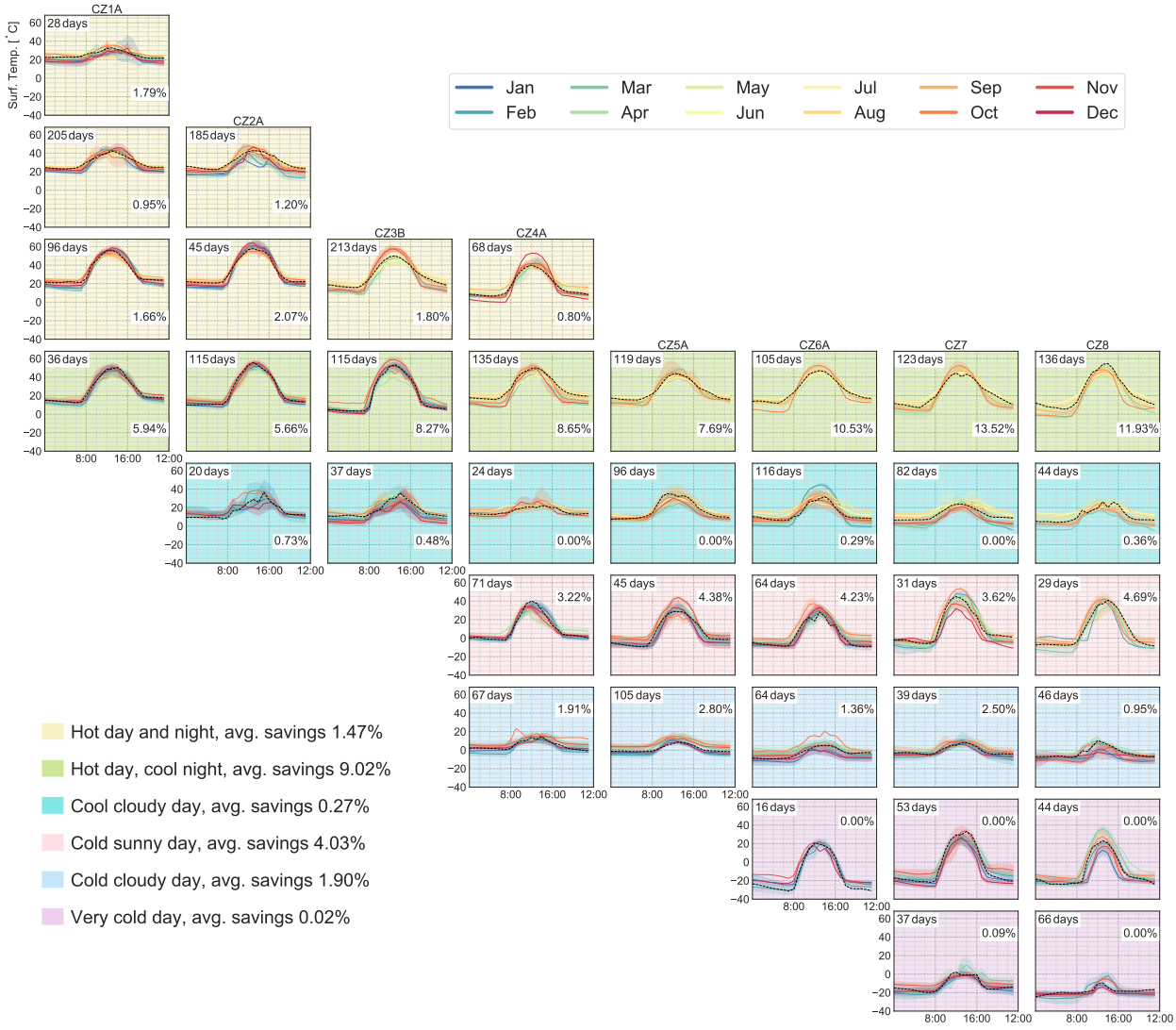

Figure 5: General visualization of the clustered days

the average savings of 9.02%. Hence, green category reveals a notable savings potential in all CZs with the fewest and the most days (i.e. 36 and 136 days) in CZ1A and CZ8, respectively. The cyan category represents cool cloudy days with little potential savings due to less cooling needs over all CZs except CZ1A with no such days in this category. Cold sunny days are shown in red and appears in CZ4A to CZ8 due to their higher heating needs than the first three CZs. The most significant savings during the heating days occurred in this category with the average savings of 4.03%. Hence, those CZs with more HDD than the CDD (Table 1) reveal a notable savings potential with the fewest and the most days (i.e. 29 and 71 days) in CZ8 and CZ4A respectively. Blue category represents cold cloudy days with less potential savings than the red category due to less solar gain. Still, with an average savings of 1.90%, blue category confirms the

ability to have savings in cloudy days in parallel to red category with sunny days. Lastly, purple represents very cold days of the year with almost no possible savings due to thermal comfort issues in CZ6A, CZ7, and CZ8.

In summary, most CZs have shown good savings potential over the course of the year in at least one of the day types. However, CZ1A with the most days in the yellow category and few cool nights had the least savings over the course of the year, whereas CZ5A with favorable conditions of cool nights in the green category and solar gains in the red category showed largest possible savings throughout the year. Overall, under the cooling condition, the green category showed the largest savings among the other categories with more ability to charge the mass during the cool nights and be then discharged during the hot days; and, under the heating condition, the red category achieved the largest savings among the other blue and purple categories. The smallest savings occurred in both the cyan category with little cooling needs and the purple category that was prone to occupant discomfort conditions.

4.2. Comparison of Savings Across Technologies

Savings across single technologies (i.e. HVAC- and AIS-only) and the merged case are illustrated in Figure 6. Each sub-figure displays the results for each CZ and the same color codes from Figure 5 are preserved. There are three line styles including dashed, solid, and dotted lines. While the first two represent the heating and cooling modes respectively, the last type suggests those days with both heating and cooling needs. Markers give more information about the row order of the corresponding clustered day from Figure 5, for referencing temperature profiles if desired. Generally, the pattern of line plots for all the clustered days show an upward savings trend from the HVAC-only technique followed by the AIS-only and the merged technique. Therefore, it confirms that buildings can benefit from the outdoor environment in both cooling and heating conditions.

In this section, we will go over each of the six categories and try to extract common or rare savings behaviors of the clustered days. The first category on the list is the yellow category representing hot days and nights with an average savings of 1.47%. This category has little opportunity to benefit from favorable ambient conditions and thus result in little savings over the CZs. In general, no technique in yellow days could surpass 2% savings and the HVAC-only technique achieved zero savings in almost all the clustered days. The only exception is with the yellow day in CZ3B where the HVAC-only technique beats the other two not only in that particular day but also among the other days in our whole study. As this day is unique, it discussed in more detail in Subsection 4.5 to understand its difference with the rest of the days in the category.

Second one the list is the green category with hot days and cool nights. Large daily temperature swings in this category enables relatively large peak demand reductions while causing small-scale energy penalty. Thus, all techniques experience their largest savings in this category with averages of 9.02%, 8.28%, and

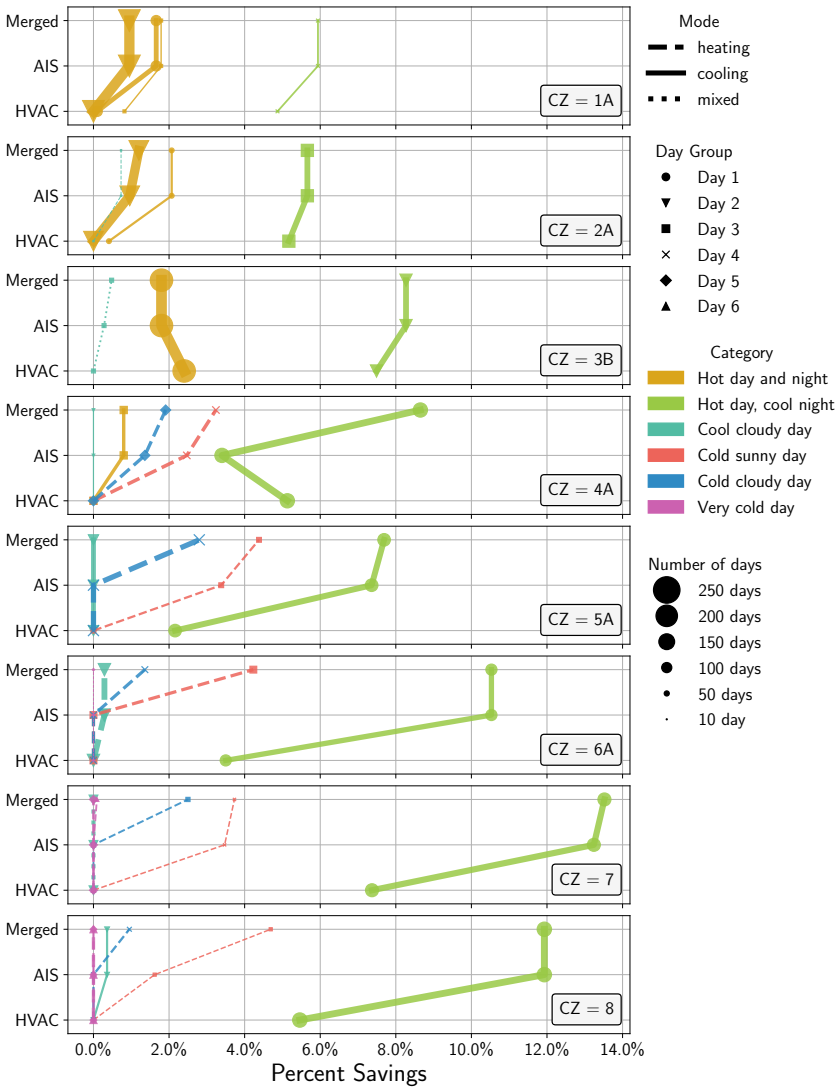

Figure 6: Savings across technologies for each clustered days in each climate zone.

5.14% for the merged, AIS-only, and HVAC-only techniques over all clustered days, respectively. Quite often, the merged technique reproduced the AIS-only technique and the optimal control causes HVAC not to perform during the peak period. Subsection 4.4 provides an example of this. While in all clustered days, the HVAC-only achieves the least savings compared to the other two techniques, the green day of CZ4A shows the AIS-only as the least achiever. Subsection 4.6 further investigates why this happened.

Cyan represents the cool cloudy days which are the low-energy days of the year. Due to minor required conditioning in this category, either cooling or heating, negligible savings is observed with no day surpassing 0.78% savings.

Next, the red category with cold sunny days shows good savings potential under heating conditions for

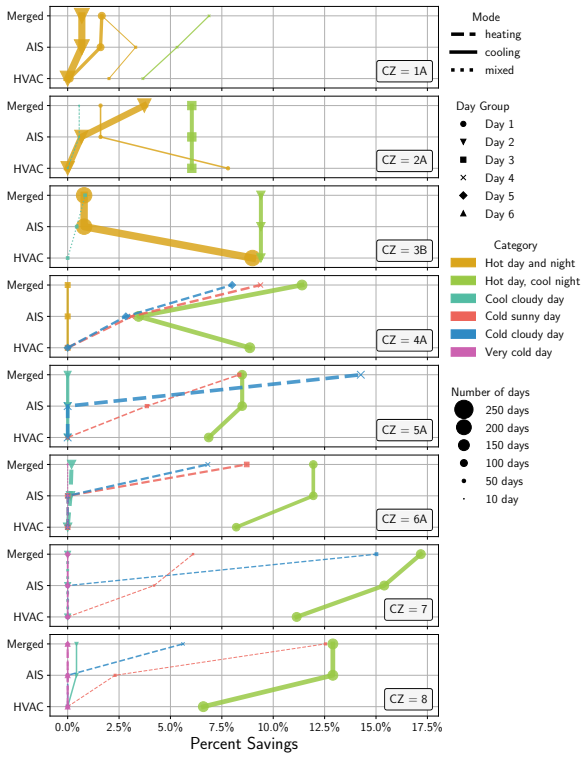

Figure 7: Peak demand savings across technologies for each clustered days in each climate zone.

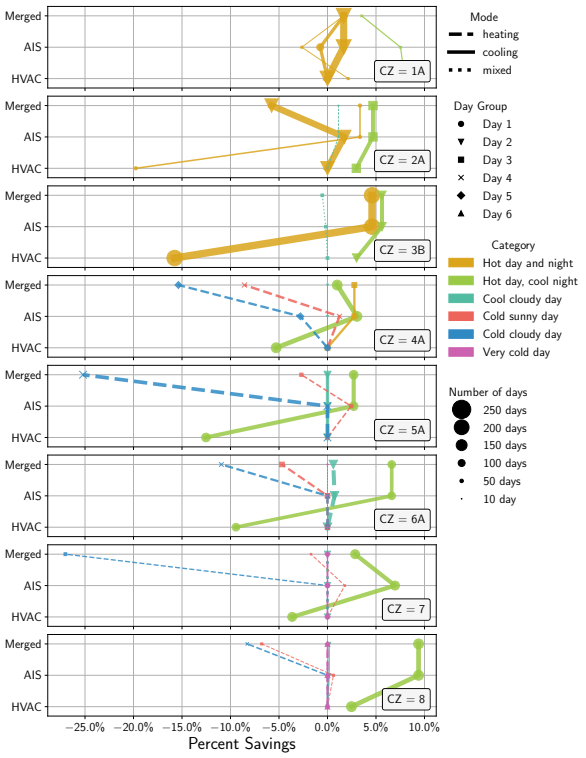

Figure 8: Energy savings across technologies for each clustered days in each climate zone.

the AIS-only and the merged techniques in all clustered days, whereas the HVAC-only achieves no savings. Optimally controlling the AIS, high solar gains in this category could charge the mass to be then used during the peak period. As a result, average savings of 4.03% and 2.19% are observed for the merged and AIS-only techniques in this category. The red day of CZ8 will be investigated in Subsection 4.4 as an example to provide more information about the beneficial solar gains in this category.

The red category is then followed by the blue category with cold cloudy days. Saving is neither observed for the AIS-only nor the HVAC-only techniques, except for in CZ 4A. Cloudy days in this category make it impossible to benefit from the sun. So, the merged technique with an average of 1.90% savings achieves half savings achieved by the red category. Lastly, the purple category with very cold days achieves no savings due to thermal comfort issues.

Unless both techniques maintained 0% savings as in the cyan and the purple categories, the AIS-only technique tended to outperformed the HVAC-only in almost all clustered days, except for the green day of CZ4A which will be discussed in Subsection 4.6. In other words, optimal control of AIS confirms the ability of buildings to advantageously utilize the outdoor weather conditions in either cooling or heating conditions. Interestingly, savings from the merged technique are similar to the AIS-only technique in most

of the clustered days. This indicated that no more savings are possible in those days and setpoint control did not add substantially more benefits to the AIS-only technique. However, there are some days with slightly more savings for the merged technique than the AIS-only, which demonstrate a complementary behavior of the savings among different techniques. Finally, a synergistic behavior is also observed in some of the clustered days including the red day of CZ8 and the green day of CZ4A. Those days will be explored in Subsections 4.4 and 4.6 respectively.

4.3. Trade-off between Peak Demand and Energy Use

Figure 7 shows amount of peak demand savings for each clustered day. Obviously, those days with high overall savings in Figure 6 also achieve large peak demand reductions. For instance, the merged technique in the green day of CZ7 has achieved the highest overall savings of 13.52% among the other clustered days in this study due to a notable peak demand savings of 17.18%, shown in Figure 7. In addition, Figure 8 shows the energy savings that also occurred for the same days. In the green day of CZ7, there were energy savings of 2.85%, showing that peak reductions were the dominant contributor to savings for the day.

Observed in Figure 7, if a day surpasses 1.66% peak demand savings, large energy penalties appear among yellow (i.e., hot) days, which results in little opportunity for this category to achieve large overall savings (shown in Figure 6). In other words, notable peak savings may be possible, but they may come at high energy penalties. For example, yellow days of CZ2A and CZ3B clearly show large energy penalties of 5.76% and 15.76% in parallel to their peak demand savings of 3.73% and 9.00%, respectively. In contrast, peak demand savings in the green category in CZ4A to CZ8 always accompany energy savings, except with the HVAC-only technique. That is, AIS-only and merged techniques in green days are highly likely to achieve both costs and energy savings at once in all CZs. The same costs and energy savings are rather clear in most of the cyan category as well.

Large peak demand savings can be achieved in both red (cold, sunny) and blue (cold, cloudy) days, however, large energy penalties go hand in hand with it on all blue days. Yet, the AIS-only technique on red days never resulted in energy penalties. Hence, the AIS-only technique in cold sunny days of the red category can achieve both costs and energy savings at once. Finally, the purple category led to no cost or energy savings due again to the earlier discomfort issues.

In several of the cases an energy penalty was noted, and hourly coefficient of performances (COP) were calculated for cooling and heating conditions to help better understand this penalty. The COPs are plotted against the outdoor drybulb temperature in Figures 9 and 10. It is rather clear from the figures that under both the cooling and heating conditions, the outdoor air temperature drastically impacts the COP of the single speed heat pump, making an inefficient situation for preconditioning the space. In other words, the single speed heat pump in this study was probably a substantial contributor to the energy penalties, as the fan and compressor cannot modulate to provide more efficient pre-cooling or pre-heating.

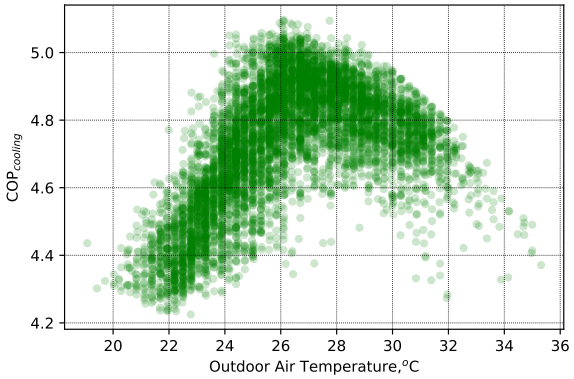

Figure 9: Variation in constant speed heat pump COP during cooling operation.

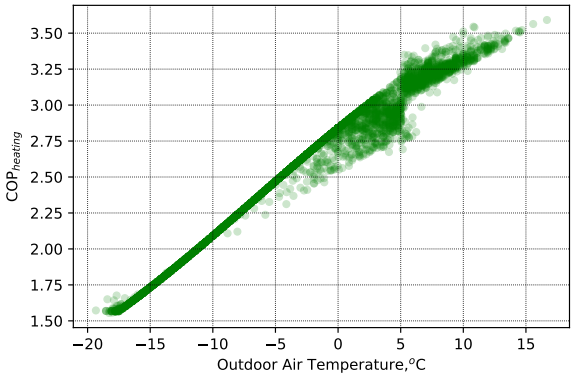

Figure 10: Variation in constant speed heat pump COP during heating operation.

4.4. Typical Savings Patterns

Following optimal control of AIS and HVAC throughout the day, a decrease can be not only observed in the peak demand but also in the energy consumption through reduction in HVAC use during the peak period. For example, Figure 11 displays how the HVAC reduction is achieved in the cooling conditions of the green day of CZ2A. Mass temperatures start from the same thermal history at the beginning of the day in the top panel, however, the bottom panel illustrates how the AIS control starts from configuration 4 to keep a warm indoor condition at the midnight and then shifts to configuration 3 from early morning to charge the mass from the cool ambient temperatures. Since then, the OPT mass temperature gradually diverges from the DEF case and thus resulted in cooler zone air temperature that barely reaches the upper limit of 24 °C in the OPT case. Configuration 3 is then followed by configuration 4 at 8 AM to keep the thermal mass temperature low enough for a discharge at configuration 2 before and during the peak period. As a result, a huge fall in the hourly power draw appears in the middle panel. To conclude, less effort of the HVAC system during on-peak hours was mainly achieved by the optimal AIS control benefiting from the large daily temperature swings of a cooling day.

While the HVAC idleness is achieved through cool ambient temperature during nighttime in a cooling day, it is achievable in a heating day through wall solar gains during daytime. For example, Figure 12 displays how the HVAC idleness is achieved in the heating conditions of the red day of CZ4A. The merged technique in this day shows a complementary behavior in its overall savings of 3.22% compared to 0.00% and 2.47% savings from HVAC-only and AIS-only techniques, respectively. From the top panel, mass temperatures start from the same thermal history at the very beginning of the day; however, it diverges from the DEF at 9 AM since AIS changes to configuration 3 in the OPT case. In other words, with no exterior insulation since sunrise, the thermal mass is charged by the solar gain. In addition, preheating the space finally leads

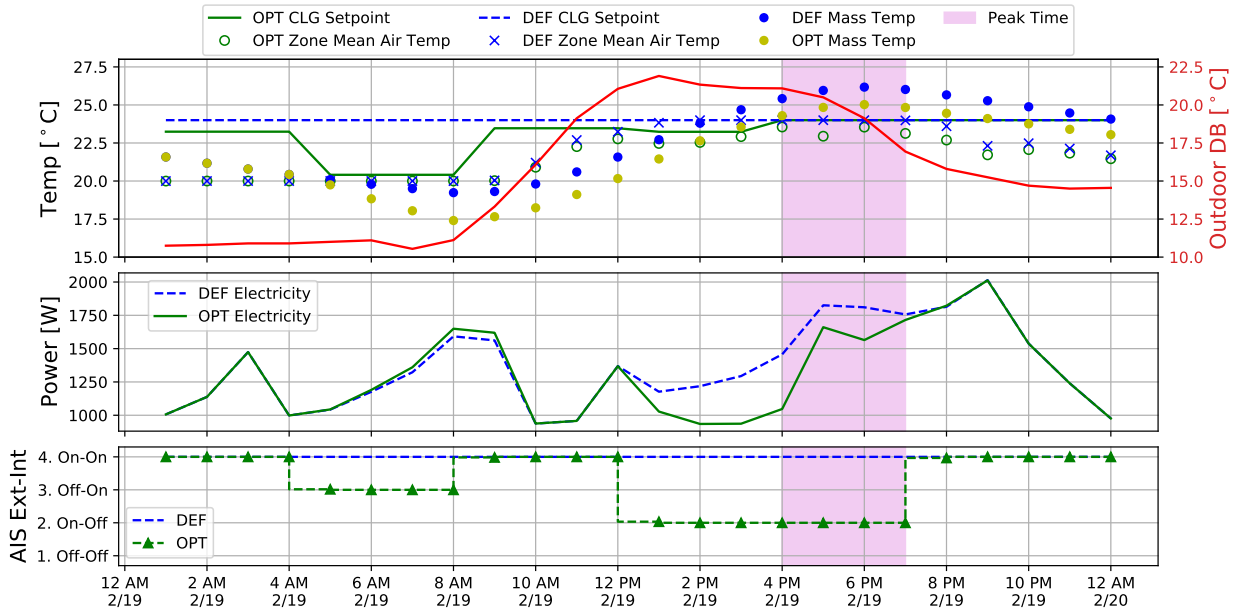

Figure 11: CZ 2A Green: Through the optimal control of HVAC and AIS, OPT zone air temperature stays within the limits for this cooling day; hence, HVAC does not need to operate during the peak period.

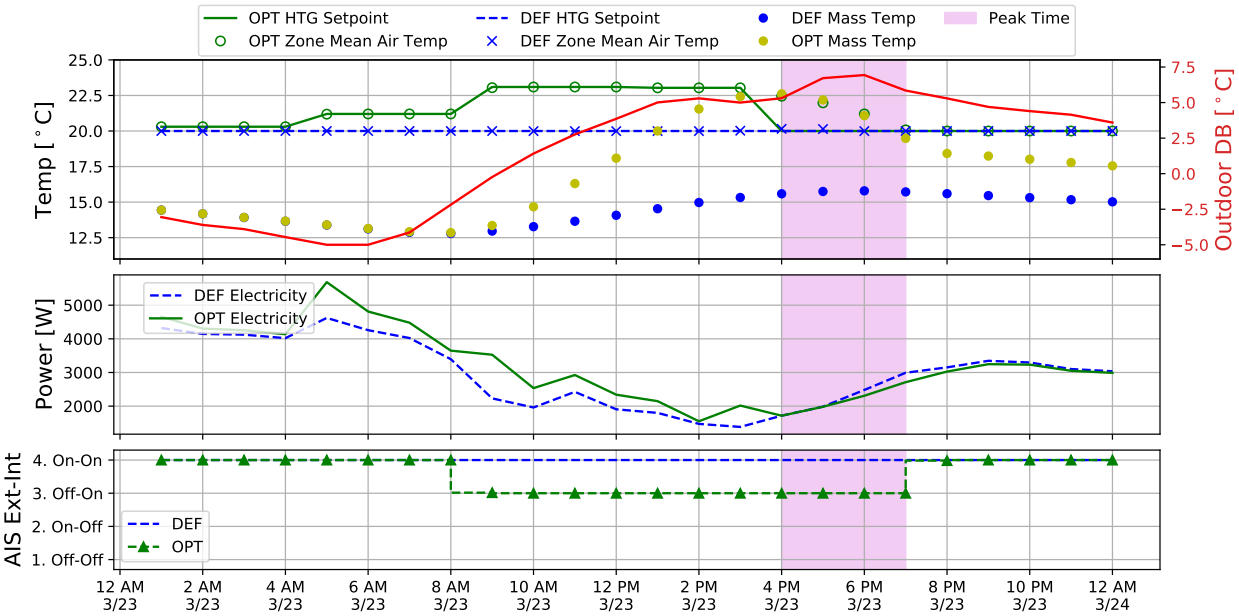

Figure 12: CZ 4A Red: Through the optimal control of HVAC and AIS, OPT zone air temperature stays within the limits for this heating day; hence, less effort is imposed on HVAC during the peak period.

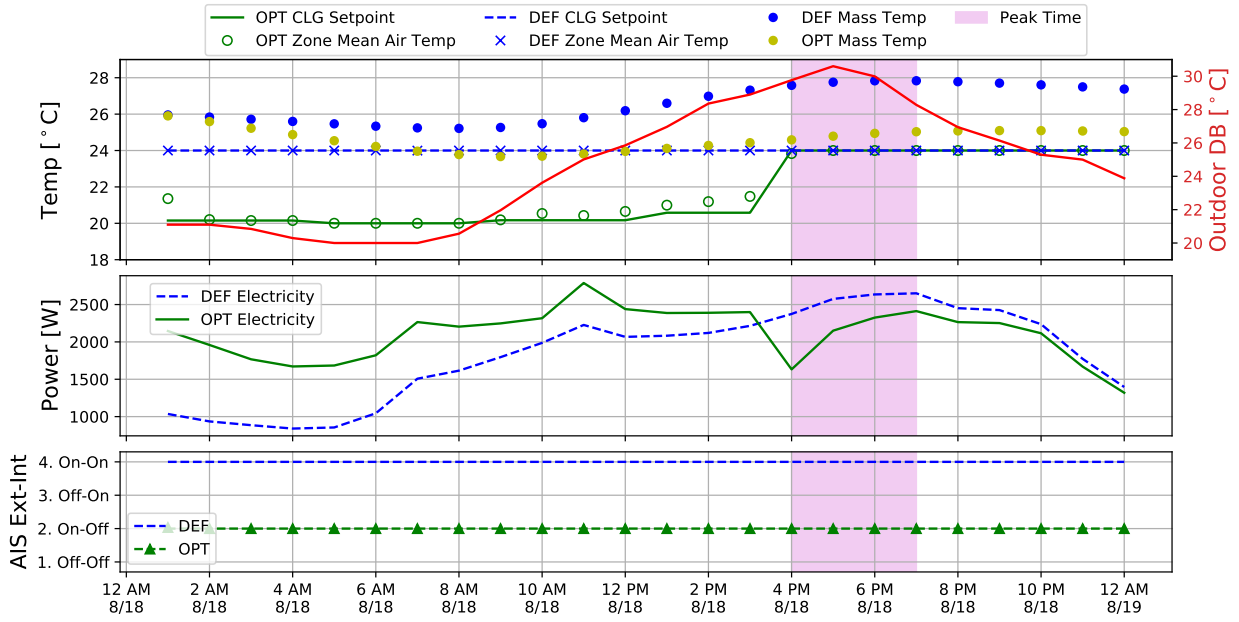

Figure 13: CZ 3B Yellow: The HVAC-only technique outperforms the other two techniques since the peak demand reduction outweighs the energy penalty as wall mass is exposed to the interior.

to higher OPT zone air temperature that remains within the limits. Hence, less power draw due to HVAC idleness during the peak period becomes apparent in the middle panel.

4.5. CZ 3B Yellow: Largest savings with HVAC-only

Excluding the green category with large daily temperature swings, the HVAC-only technique, in general, causes little to no savings as a consequence of large energy penalties. According to Figure 6, the HVAC-only technique reaches the highest savings among the other two techniques only in one clustered day (i.e. yellow day of CZ3B). Figure 13 displays details of that day in three panels displaying relevant temperature trajectories (i.e., cooling setpoint, zone air temperature, and mass temperature for both default (DEF) and optimum (OPT) cases on the left axis, and outdoor drybulb on the right axis) in the top panel, total building power draw in the middle panel, and AIS control in the bottom panel. Note that although the merged technique is at least able to reproduce the optimal solution of the AIS-only technique, it is not capable of reproducing the optimal solution of the HVAC-only technique since the HVAC-only uses wall configuration 5 (Subsection 3.1) to evaluate the full power of HVAC-only technique if all mass is exposed to the indoor zone while the required R-value is satisfied only at the exterior insulation layer.

Mass temperatures start from the same thermal history at the beginning of the day; however, adjusting the setpoint at 20 °C for the OPT case, the space is preconditioned, and OPT mass temperature diverges from the DEF mass temperature gradually until the maximum difference of 3 °C happens during the peak

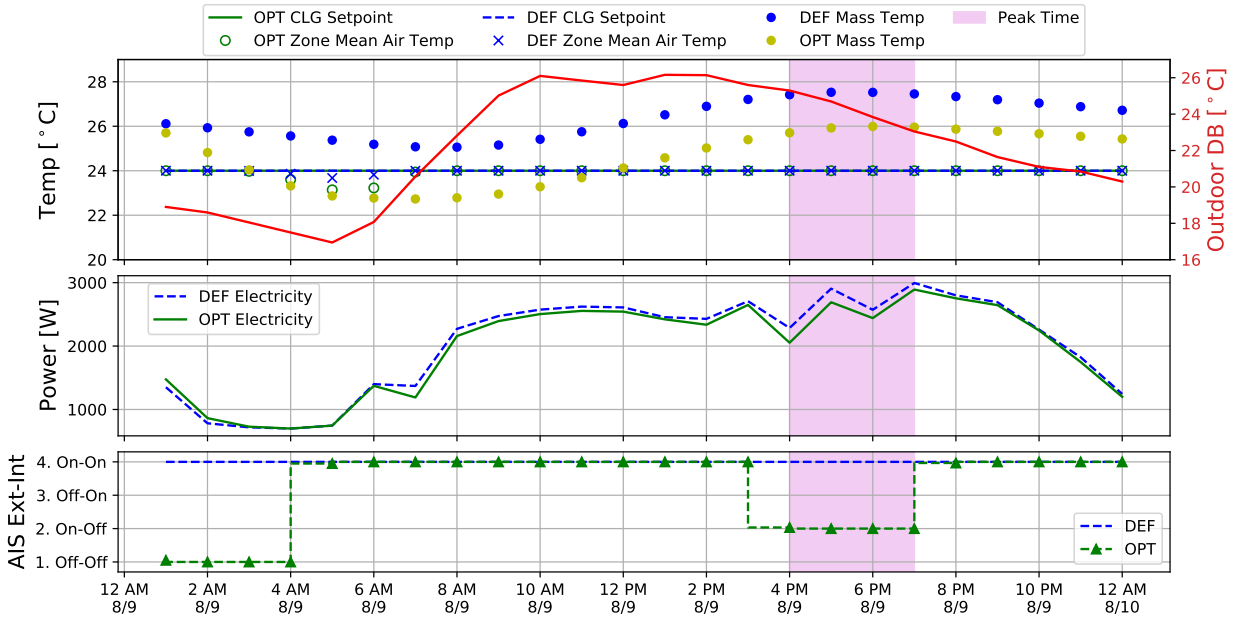

Figure 14: CZ4A Green: The AIS-only technique is overcome by the other two techniques since it was not able to store as much thermal energy to reduce the afternoon peak.

time. That is, construction mass is charged during off-peak, and then discharged during the on-peak period. The middle panel compares hourly power draws of the building with the highest DEF peak of 2.68 kW happening at 6 pm. From this panel, a clear peak demand reduction of about 10% is obvious from 2.65 kW to 2.41 kW while increasing the overall energy consumption by about 16%, which can be understood from the area under the curves. However, the overall savings in this day is 2.40% which appeared to be larger than the overall savings of 1.80% in the AIS-only and the merged techniques. The bottom panel displays no AIS optimization in this test and both the baseline and HVAC-only case studies remain at constant controls of 4 and 5, respectively. As mentioned in the Methods section, configuration 5 is only used in this test since it allows for assessing the full capability of the HVAC system to lower the cost function by charging the thermal mass from the interior, while satisfying the total R-value requirement.

4.6. CZ 4A Green: Least savings with AIS-only

Results for the AIS-only case study are compared to the baseline in Figure 14. From the top panel, mass temperatures start from the same thermal history at the very beginning of the day; however, it diverges from the DEF since AIS is at configuration 1 in the OPT case. In other words, no insulation lets the thermal mass be charged by the cool ambient air in the nighttime to be then discharged later in the day. The bottom panel illustrates how the AIS control starts from configuration 1 to decrease the thermal mass temperature; followed by 4 to keep the thermal mass temperature low enough for a discharge at configuration 2 in the

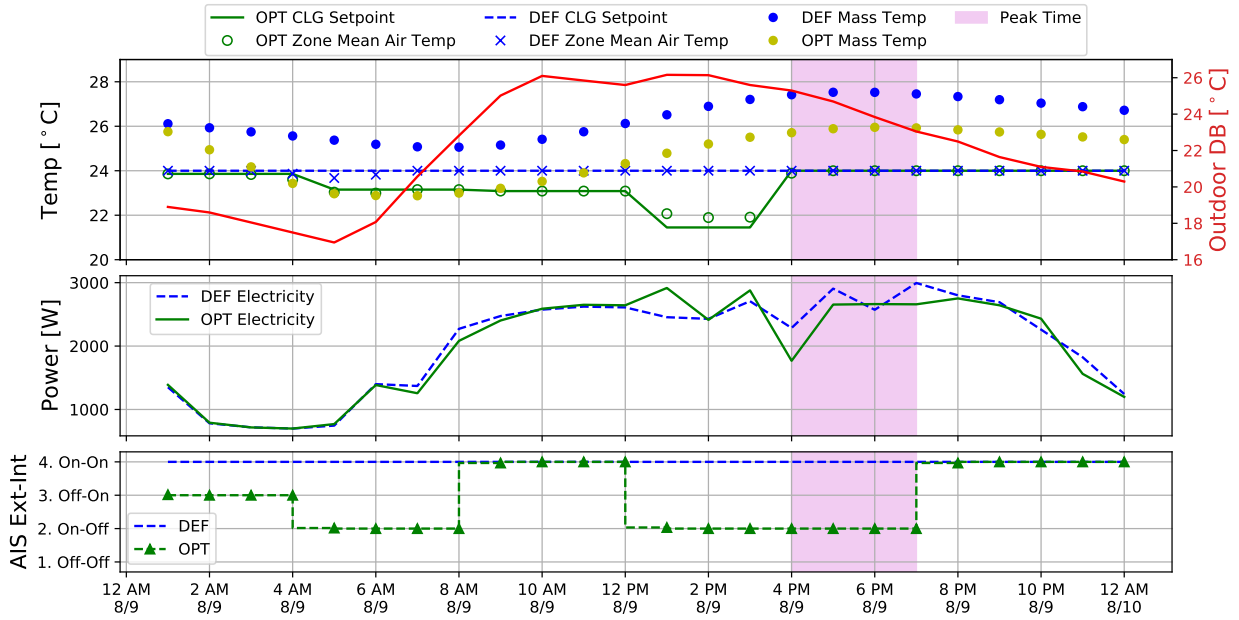

Figure 15: CZ4A Green: The merged technique shows synergistic savings of 8.65% due to the larger peak demand reduction.

peak period. The middle panel compares hourly power draws of the building with the highest DEF peak of 2.99 kW happening at 7 pm. From this panel, a clear peak demand reduction of 3% is obvious from 2.99 kW to 2.89 kW while decreasing the overall energy consumption by 3%, which can be understood from the area under the curves.

Despite the poor performance of the AIS-only technique in reducing the peak demand in the green day of CZ4A, the merged case with the overall savings of 8.65% showed an unique synergistic behavior compared to the savings of the HVAC-only and AIS-only techniques with 5.13% and 3.34%, respectively. Results for the merged case in that green day are compared to the baseline in Figure 15. From the top panel, mass temperatures start from the same thermal history at the very beginning of the day; however, it diverges from DEF since AIS starts at configuration 3 and the CLG setpoint is allowed to be lower than 24 °C in the OPT case. Differences were subtle but due to the different AIS control besides the HVAC precooling, the merged technique led to lower OPT zone air temperature before the peak and lower OPT mass temperature from 2 to 5 pm which enabled more charging of the mass compared to the AIS-only technique. Also, charging the mass when the outdoor DB was about 26 °C, the merged technique benefited from a more efficient cooling system before the peak in contrast to the cooling system in the AIS-only technique that primarily run when the outdoor DB was decreasing by multiple degrees from 26 °C. Consequently, the merged technique was more successful in reducing the peak by 11% from 2.99 kW to 2.66 kW while decreasing the overall energy consumption by 2%.

5. Conclusions, Limitations, and Future Work

This article extends our previous analysis [35] to a more comprehensive examination that considers the AIS and HVAC control optimizations in different climate zones, and for annual variation in weather data. For baseline prototype buildings in each CZ, time series clustering problems were solved on the outside surface temperature which was believed to be the best indicator of the potential for utilizing AIS. Applying a RMSE evaluation, centroid days were found in each cluster and optimization problems were then solved on those centroid days to determine the potential savings for each cluster. Results revealed common weather conditions among different CZs, which led to advent of color codes to distinguish different savings behaviors. For instance, under the cooling conditions, yellow category represents the days with high temperatures during both the daytime hours and nighttime hours, which appear in decreasing numbers from CZ1A to CZ4A. While the average savings in that category was as little as 1.47%, green category (hot day, cool night) with large daily temperature swings achieved a high average of 9.02%. In the opposite, under the heating conditions, the red category (cold sunny day) benefited from high solar gains and achieved an average savings of 4.03%. Then, the blue category (cold cloudy day) was less successful to save with 1.90%. Cool cloudy days and very cold days known as cyan and purple categories in this study have shown little to no savings due to the light required conditioning in the former and thermal comfort issues in the latter.

The cost function used in this study considered a 70%-30% weighting for the peak demand and the daily energy consumption, respectively. That is, overall savings can be achieved relatively more by reducing the peak demand than minimizing the energy consumption. Hence, often, there were cases with less peak demand and more energy consumption. No demand limit was targeted in this study, however, after a thorough investigation of different weightings, the 70%-30% appeared to be heavy enough to demonstrate a good ability to penalize inefficient charging of the building mass, leading to peak demand reductions and energy savings, when possible.

In an intricate comparison of savings across single technologies (HVAC and AIS-only) and the merged case, typical patterns were observed and discussed throughout this study. While the HVAC-only technique achieved the least savings in all color codes, the merged technique usually reproduced the same results as the AIS-only technique, indicating that the AIS system achieved the full capacity in most clustered days and HVAC preconditioning could add no more benefit. According to the hourly mass temperature profiles under the cooling conditions, those savings were due to the construction thermal storage that could be charged during cool nighttime outdoor and discharged during the hot daytime environment as well as maintaining the indoor air temperature within the limits by precooling, which led to HVAC idleness during the peak period. Similarly, under the heating conditions, less effort was set on HVAC, this time due to the construction thermal storage that could be charged during sunny days in parallel to HVAC preheating.

Typically, the peak demand reduction through the HVAC-only technique was always accompanied with

large energy penalty and thus made this technique less favorable compared to the other two techniques. However, an anomaly was observed in the pattern of a yellow day in CZ3B that experienced its largest savings from the HVAC-only technique. Exceptionally in that day, the peak demand reduction outweighed energy penalty and resulted in the highest savings among the other two techniques. Also, another anomaly was observed in the pattern of a green day in CZ4A with the least savings from the AIS-only technique. In that day, the HVAC-only was more successful in reducing the peak demand than the AIS-only since, similar to the previous anomaly, the peak demand reduction outweighed accompanying energy penalty. This time though, the merged technique did not reproduce the AIS-only results, instead it showed a synergistic behavior for the savings.

Although a couple of anomalies appeared in the savings patterns, the merged technique could at least reproduce the same savings as the AIS-only technique in one day and reach even a far larger savings in the other one. Overall, the results assures how active envelope, HVAC control, and building thermal storage can work together to achieve both flexibility (e.g., load shifting) and efficiency. Consequently, GEBs employing active insulation, intelligent HVAC controls, and thermal storage can contribute to greater affordability and reliability of the power system, reductions in greenhouse gas emissions through lower energy consumption, and more renewable energy integration through their flexibility.

The AIS and HVAC control essentially provides two mechanisms for charging the same envelope thermal mass, thus, there are limitations on how much energy can be stored and how quickly the mass can be charged and discharged. Future work could consider buildings with more mass and integration of phase change materials and/or active thermal storage with active envelopes to explore optimal system designs that improve upon these initial results. Executing the joint optimization with detailed whole building models was a computationally intensive task and a limitation in our previous study [35]. Thus, this work used clustering methods to explore the savings potential for a full year through the use of representative day types. The clustering problems also enabled considering prototype buildings with different insulation levels and in different climate zones. However, the largest limitation of this study is perhaps that the AIS configuration was controlled in all the surrounding walls at once. In the future, this work will be expanded further to examine the joint optimization of HVAC and AIS controls in separate walls.

Bibliography

[1] Energy efficiency – topics - iea. 2021. URL: https://www.iea.org/topics/energy-efficiency.

[2] DOE U. Chapter 5: Increasing efficiency of building systems and technologies. Quadrennial Technology Review: An Assessment of Energy Technologies and Research Opportunities 2015;:143–81.

[3] Satchwell A, Piette MA, Khandekar A, Granderson J, Frick NM, Hledik R, et al. A national roadmap for grid-interactive efficient buildings. Tech. Rep.; Lawrence Berkeley National Lab.(LBNL), Berkeley, CA (United States); 2021.

[4] Shekar V, Krarti M. Control strategies for dynamic insulation materials applied to commercial buildings. Energy and

Buildings 2017;154:305–20. URL: https://doi.org/10.1016/j.enbuild.2017.08.084. doi:10.1016/j.enbuild.2017.08.084.

[5] Cui B, Dong J, Lee S, Im P, Salonvaara M, Hun D, et al. Model predictive control for active insulation in building envelopes. Energy and Buildings 2022;267:112108. URL: https://www.sciencedirect.com/science/article/pii/S0378778822002791. doi:https://doi.org/10.1016/j.enbuild.2022.112108.

[6] Braun JE. Reducing energy costs and peak electrical demand through optimal control of building thermal storage. ASHRAE transactions 1990;96(2):876–88.

[7] Rabl A, Norford L. Peak load reduction by preconditioning buildings at night. International Journal of Energy Research 1991;15(9):781–98.

[8] Morris F, Braun JE, Treado S. Experimental and simulated performance of optimal control of building thermal storage. Ashrae transactions 1994;100(1):402–14.

[9] Keeney KR, Braun JE. Application of building precooling to reduce peak cooling requirements. ASHRAE transactions 1997;103(1):463–9.

[10] Florita AR, Cheng H, et al. Optimization of building thermal mass control in the presence of energy and demand charges. ASHRAE Transactions 2008;114:75.

[11] Drgoňa J, Arroyo J, Figueroa IC, Blum D, Arendt K, Kim D, et al. All you need to know about model predictive control for buildings. Annual Reviews in Control 2020;50:190–232.

[12] Ma J, Qin SJ, Li B, Salsbury T. Economic model predictive control for building energy systems. IEEE; 2011.

[13] Greensfelder EM, Henze GP, Felsmann C. An investigation of optimal control of passive building thermal storage with real time pricing. Journal of Building Performance Simulation 2011;4(2):91–104.

[14] Olivieri SJ, Henze GP, Corbin CD, Brandemuehl MJ. Evaluation of commercial building demand response potential using optimal short-term curtailment of heating, ventilation, and air-conditioning loads. Journal of Building Performance Simulation 2014;7(2):100–18.

[15] Arroyo J, Spiessens F, Helsen L. Comparison of model complexities in optimal control tested in a real thermally activated building system. Buildings 2022;12(5):539.

[16] De Coninck R, Helsen L. Practical implementation and evaluation of model predictive control for an office building in brussels. Energy and Buildings 2016;111:290–8.

[17] Henze GP. Model predictive control for buildings: a quantum leap? 2013.

[18] Larsen TS, Jensen RL. Comparison of measured and calculated values for the indoor environment in one of the first Danish passive houses. Proceedings of Building Simulation 2011: 12th Conference of International Building Performance Simulation Association 2011;:1414–21.

[19] McLeod RS, Hopfe CJ, Kwan A. An investigation into future performance and overheating risks in Passivhaus dwellings. Building and Environment 2013;70:189–209. URL: http://dx.doi.org/10.1016/j.buildenv.2013.08.024. doi:10.1016/j.buildenv.2013.08.024.

[20] Chvatal KMS, Corvacho H. The impact of increasing the building envelope insulation upon the risk of overheating in summer and an increased energy consumption. Journal of Building Performance Simulation 2009;2(4):267–82. doi:10.1080/19401490903095865.

[21] Park B, Srubar WV, Krarti M. Energy performance analysis of variable thermal resistance envelopes in residential buildings. Energy and Buildings 2015;103:317–25. URL: http://dx.doi.org/10.1016/j.enbuild.2015.06.061. doi:10.1016/j.enbuild.2015.06.061.

[22] Kishore RA, Bianchi MV, Booten C, Vidal J, Jackson R. Enhancing building energy performance by effectively using phase change material and dynamic insulation in walls. Applied Energy 2021;283(November 2020):116306. URL: https://doi.org/10.1016/j.apenergy.2020.116306. doi:10.1016/j.apenergy.2020.116306.

[23] Kimber M, Clark WW, Schaefer L. Conceptual analysis and design of a partitioned multifunctional smart insulation. Applied Energy 2014;114:310–9. URL: http://dx.doi.org/10.1016/j.apenergy.2013.09.067. doi:10.1016/j.apenergy.2013.09.067.

[24] Imbabi MSE. A passive–active dynamic insulation system for all climates. International Journal of Sustainable Built Environment 2012;1(2):247–58. doi:10.1016/j.ijsbe.2013.03.002.

[25] Pflug T, Kuhn TE, Nörenberg R, Glück A, Nestle N, Maurer C. Closed translucent façade elements with switchable U-value - A novel option for energy management via the facade. Energy and Buildings 2015;86:66–73. URL: http://dx.doi.org/10.1016/j.enbuild.2014.09.082. doi:10.1016/j.enbuild.2014.09.082.

[26] Pflug T, Bueno B, Siroux M, Kuhn TE. Potential analysis of a new removable insulation system. Energy and Buildings 2017;154:391–403. URL: https://doi.org/10.1016/j.enbuild.2017.08.033. doi:10.1016/j.enbuild.2017.08.033.

[27] Pflug T, Nestle N, E. Kuhn T, Siroux M, Maurer C. Modeling of facade elements with switchable U-value. Energy and Buildings 2018;164:1–13. URL: https://doi.org/10.1016/j.enbuild.2017.12.044. doi:10.1016/j.enbuild.2017.12.044.

[28] Varga S, Oliveira AC, Afonso CF. Characterisation of thermal diode panels for use in the cooling season in buildings. Energy and Buildings 2002;34(3):227–35. doi:10.1016/S0378-7788(01)00090-1.

[29] Benson DK, Potter TF, Tracy CE. Design of a variable-conductance vacuum insulation. SAE Technical Papers 1994;103(1994):176–81. doi:10.4271/940315.

[30] Favoino F, Jin Q, Overend M. Design and control optimisation of adaptive insulation systems for office buildings. Part 1: Adaptive technologies and simulation framework. Energy 2017;127:301–9. URL: http://dx.doi.org/10.1016/j.energy.2017.03.083. doi:10.1016/j.energy.2017.03.083.

[31] Jin Q, Favoino F, Overend M. Design and control optimisation of adaptive insulation systems for office buildings. Part 2: A parametric study for a temperate climate. Energy 2017;127:634–49. URL: http://dx.doi.org/10.1016/j.energy.2017.03.096. doi:10.1016/j.energy.2017.03.096.

[32] Menyhart K, Krarti M. Potential energy savings from deployment of Dynamic Insulation Materials for US residential buildings. Building and Environment 2017;114:203–18. URL: http://dx.doi.org/10.1016/j.buildenv.2016.12.009. doi:10.1016/j.buildenv.2016.12.009.

[33] Antretter F, Cui B, Hun D, Boudreaux P. Assessing the potential of active insulation systems to reduce energy consumption and enhance electrical grid services. Thermal Performance of the Exterior Envelopes of Whole Buildings 2019;.

[34] Mumme S, James N, Salonvaara M, Shrestha S, Hun D. Smart and efficient building envelopes: Thermal switches and thermal storage for energy savings and load flexibility. ASHRAE Transactions 2020;126:140–8.

[35] Sepehri A, Pavlak G. Joint optimization of hvac and active insulation control strategies in residential buildings. ASHRAE Annual Conference 2022;.

[36] Energy star degree day calculator. 2019. URL: https://portfoliomanager.energystar.gov/pm/degreeDaysCalculator.

[37] Oceanic TN, (NOAA) AA. U.s. climate normals quick access. 2006-2020. URL: https://www.ncei.noaa.gov/.

[38] pyswarms.single package — pyswarms 1.3.0 documentation. 2017. URL: https://pyswarms.readthedocs.io/en/latest/api/pyswarms.single.html#module-pyswarms.single.local_best.

[39] Energyplus eppy. 2021. URL: https://eppy.readthedocs.io/en/latest/readme.html.